RAS-converting enzyme 1-mediated endoproteolysis is required for trafficking of rod phosphodiesterase 6 to photoreceptor outer segments

Jeffrey R. Christiansen[a,b], Saravanan Kolandaivelu[a,b,c], Martin O. Bergo[d], and Visvanathan Ramamurthy[a,b,c,1]

[a]Center for Neuroscience and Departments of [b]Ophthalmology and [c]Biochemistry, Robert C. Byrd Health Sciences Center, West Virginia University, Morgantown, WV 26505; and [d]Cancer Center Sahlgrenska, University of Gothenburg, SE 413 45 Gothenburg, Sweden

Edited by Jeremy Nathans, The Johns Hopkins University, Baltimore, MD, and approved April 13, 2011 (received for review March 15, 2011)

Prenylation is the posttranslational modification of a carboxyl-terminal cysteine residue of proteins that terminate with a CAAX motif. Following prenylation, the last three amino acids are cleaved off by the endoprotease, RAS-converting enzyme 1 (RCE1), and the prenylcysteine residue is methylated. Although it is clear that prenylation increases membrane affinity of CAAX proteins, less is known about the importance of the postprenylation processing steps. RCE1 function has been studied in a variety of tissues but not in neuronal cells. To approach this issue, we generated mice lacking *Rce1* in the retina. Retinal development proceeded normally in the absence of *Rce1*, but photoreceptor cells failed to respond to light and subsequently degenerated in a rapid fashion. In contrast, the inner nuclear and ganglion cell layers were unaffected. We found that the multimeric rod phosphodiesterase 6 (PDE6), a prenylated protein and RCE1 substrate, was unable to be transported to the outer segments in *Rce1*-deficient photoreceptor cells. PDE6 present in the inner segment of *Rce1*-deficient photoreceptor cells was assembled and functional. Synthesis and transport of transducin, and rhodopsin kinase 1 (GRK1), also prenylated substrates of RCE1, was unaffected by *Rce1* deficiency. We conclude that RCE1 is essential for the intracellular trafficking of PDE6 and survival of photoreceptor cells.

protein posttranslational modification | protein transport | retinal degeneration | methyl esterification

Posttranslational modifications increase a protein's functional repertoire, regulating protein–protein interactions and targeting to cellular components. One such posttranslational modification is prenylation, a three-step process that first adds a farnesyl or geranylgeranyl lipid to the C-terminal cysteine of proteins ending in a CAAX motif (C, cysteine; A, aliphatic amino acid; X, any amino acid residue) (1–3). The next step is proteolysis of the last three amino acids (-AAX) by the protease RAS-converting enzyme 1 (RCE1) or zinc metalloproteinase sterile-24 homologue (ZMPSTE24) (4, 5). The final step is the methyl esterification of the newly exposed isoprenylcysteine residue catalyzed by isoprenylcysteine carboxyl methyltransferase (ICMT) (4).

Prenylation enables peripheral membrane proteins to interact with membranes and facilitates their interaction with protein partners (2). The significance of the proteolysis and methylation steps is not entirely clear (4). In general, farnesylated proteins require postprenylation processing for proper localization, whereas the more hydrophobic geranylgeranylated proteins do not (6). Germline knockout of *Rce1* or *Icmt* results in embryonic lethality in mice, demonstrating the importance of these processing steps during development (7, 8). Subsequent conditional knockout studies revealed that proteolysis is crucial in the heart but is dispensable in liver and bone marrow (9, 10). Although *Rce1* is expressed in the brain and eye, the role of RCE1-mediated endoproteolysis in neuronal tissue in vivo is not known (7).

Several phototransduction signaling proteins in the retina are prenylated RCE1 substrates. These proteins include transducin (Tγ), rhodopsin kinase (GRK1), and phosphodiesterase 6 (PDE6) catalytic subunits (αβ) (11–16). Transducin, a heterotrimeric G protein in the photoreceptor cells, relays the light response from the activated G protein coupled receptor rhodopsin to the effector enzyme PDE6 (17). The transducin heterotrimer consists of a myristoylated $G_{\alpha t1}$ subunit (Tα), a $G_{\beta 1}$ subunit (Tβ), and a farnesylated $G_{\gamma 1}$ subunit (14). In vitro studies show that methyl esterification of $G_{\gamma 1}$ is required for efficient assembly of the heterotrimer as well as targeting to the plasma membrane (18, 19).

PDE6 is the phototransduction effector enzyme that hydrolyzes cGMP to GMP in response to light-activated transducin (17). Rod PDE6 heterotetramer is composed of catalytic α- and β-subunits and two inhibitory γ-subunits (20). A unique feature of PDE6 is the differential prenylation of catalytic subunits: the α-subunit is farnesylated and the β-subunit geranylgeranylated (15). In contrast, the catalytic subunit of cone PDE6, a homodimer is thought to be geranylgeranylated (20). The importance of PDE6 prenylation in retinal function is implied by studies on a canine model for retinitis pigmentosa (21). The disease is caused by a nonsense mutation in PDE6 that truncates the C-terminal 49 aa residues including the CAAX box. This results in an unstable protein and leads to degeneration of photoreceptor cells (21). Lack of a functional heterologous expression system and suitable animal models has hampered the in-depth analysis needed to understand the role of postprenylation processing in PDE6 function (22).

The role of prenylation and methyl esterification of proteins in the maintenance of retinal neurons has been investigated by injecting lovastatin, an inhibitor of HMG-CoA reductase, and *N*-acetyl-S-farnesyl-L-cysteine, an inhibitor of ICMT, into the eye (23). After 4 d, the retinas were severely disorganized and formed rosette-like structures (23). However, the results of the study are confounded by the fact that lovastatin and *N*-acetyl-S-farnesyl-L-cysteine may also affect endothelial cells in blood vessels, leading to apoptosis of photoreceptor cells (24). Consistent with this idea, blood vessel shunting was observed in injected eyes (23).

To define the importance of postprenylation processing of CAAX proteins in the eye, we used a genetic approach to eliminate RCE1-mediated proteolysis and subsequent methyl esterification specifically in retinal neurons. To accomplish this, we bred conditional *Rce1*-KO mice on a background of a retina-specific *Cre* transgene and analyzed the impact of *Rce1* deficiency in retinal neurons.

Author contributions: J.R.C. and V.R. designed research; J.R.C. and S.K. performed research; M.O.B. contributed new reagents/analytic tools; J.R.C. and V.R. analyzed data; and J.R.C., M.O.B., and V.R. wrote the paper.

The authors declare no conflict of interest.

This article is a PNAS Direct Submission.

[1]To whom correspondence should be addressed. E-mail: ramamurthyv@wvuhealthcare.com.

This article contains supporting information online at www.pnas.org/lookup/suppl/doi:10.1073/pnas.1103627108/-/DCSupplemental.

Results

Generation of Mice Lacking *Rce1* in the Retina. To eliminate *Rce1* expression in the retina, we used mice carrying the conditional $Rce1^{fl}$ allele and the *Six3-Cre* transgene mice, which express Cre recombinase in cells of the nascent neural retina beginning at embryonic day 10 (25, 26). The efficiency of Cre recombination was assessed by breeding the *Six3-Cre* mice with a tdTomato reporter line (Fig. S1) (27). Uniform expression of tdTomato was observed throughout all cell layers in retinas of adult mice, demonstrating efficient Cre-mediated recombination. We bred $Rce1^{wt/null}$*Six3-Cre* males with $Rce1^{fl/fl}$ females to generate $Rce1^{fl/null}$*Six3-Cre* mice (designated $Rce1^{-/-}$). Littermate $Rce1^{fl/wt}$*Six3-Cre*, $Rce1^{fl/wt}$, and $Rce1^{fl/null}$ mice (collectively designated $Rce1^{+/-}$) were indistinguishable from WT mice and were used as controls. $Rce1^{+/-}$ and $Rce1^{-/-}$ littermates did not differ in size, mortality, or gross eye morphology.

Rce1 expression in retinas of $Rce1^{-/-}$ mice was reduced by 90% as judged by quantitative PCR (Fig. 1*A*). The expression of *Zmpste24*, a related endoprotease, which served as a control, was similar in $Rce1^{+/-}$ and $Rce1^{-/-}$ retinas (Fig. 1*A*).

RCE1-Mediated Endoproteolysis Is Required for Viability of Photoreceptor Cells. To determine if the development of the laminated cell layers of the retina was affected by *Rce1* deficiency, we examined retinal morphology by using semithin plastic sections stained with H&E from postnatal day (P) 8 and P16 $Rce1^{+/-}$ and $Rce1^{-/-}$ mice. At P8, we observed similar numbers of nuclei in all three cell layers (outer, inner, and ganglion) in $Rce1^{+/-}$ and $Rce1^{-/-}$ retinas and no signs of cell death (Fig. 1*B* and Fig. S2). Both rod and cone photoreceptor cells were present (Fig. S3). At P16, however, the number of photoreceptor cell nuclei was dramatically reduced (Fig. 1*B*). This reduction was limited to the outer nuclear layer (ONL), as the thickness of the inner and ganglion cell layers was unaltered. Indeed, no cell death or reduction in cell numbers was observed in the inner and ganglion layer up to 1 y of age (Fig. S2). The development and survival of horizontal, amacrine, and ganglion cells was unaffected by *Rce1* deficiency as judged by immunostaining of P30 retinal cryosections (Fig. S4). We conclude that *Rce1* is dispensable for the development of retinal neurons but required for the subsequent viability of photoreceptor cells.

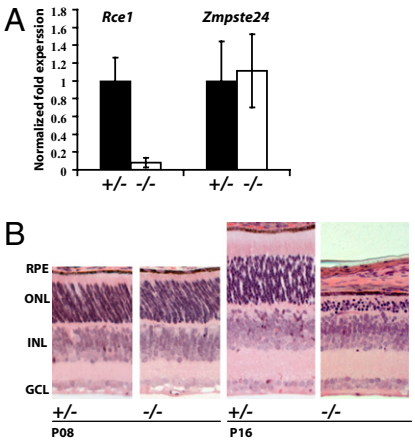

Fig. 1. Elimination of *Rce1* in the retina leads to rapid photoreceptor cell degeneration. (*A*) RT-PCR from P8 retinal cDNA with primers for *Rce1 and Zmpste24* normalized to *Hprt.* (*B*) Semithin plastic sections of P08 and P16 $Rce1^{+/-}$ and $Rce1^{-/-}$ littermates were stained with H&E and imaged on an Olympus AX70 epifluorescent/transmitted light microscope. RPE, retinal pigment epithelium; INL, inner nuclear layer; GCL, ganglion cell layer.

***Rce1* Deficiency Reduces Light-Evoked Responses.** We performed electroretinography (ERG) to evaluate light responses of *Rce1*-deficient photoreceptor cells. The *a*-wave of an ERG is generated by the collective response of photoreceptor cells in response to a flash of light. This is followed by a *b*-wave, which is primarily shaped by response from bipolar cells (28). Scotopic (rod-mediated) conditions produced robust *a*- and *b*-waves in P14 $Rce1^{+/-}$ mice at various light intensities (Fig. 2*A*). Photopic (i.e., cone-mediated) conditions also produced a characteristic *b*-wave in $Rce1^{+/-}$ mice (Fig. 2*B*). In contrast, recordings from $Rce1^{-/-}$ mice failed to produce measurable *a*-waves under any illumination condition and only minimal *b*-wave responses (Fig. 2 *A* and *B*). In agreement with the morphological analysis, which showed complete degeneration of photoreceptor cells, light-evoked responses were also abolished at P35 (Fig. S5). Collectively, these results demonstrate that *Rce1* is required for the proper function of photoreceptor cells.

Absence of RCE1-Mediated Proteolytic Cleavage Does Not Affect the Stability of Prenylated Photoreceptor Cell Proteins. The ERG results suggest that the absence of *Rce1* affects proteins involved in the light response. Therefore, we examined the levels of prenylated proteins involved in phototransduction (Fig. 3*A*). We reasoned that a major destabilization and degradation of either Tγ or PDE6 could lead to the loss of function we observed, similar to the knockout of either of these genes (29, 30). However, the levels of Tγ, PDE6αβ, cone PDE6α′, and GRK1 in P8 retinal homogenates, before any detectable cell death, was similar in $Rce1^{+/-}$ and $Rce1^{-/-}$ retinas (Fig. 3*A*). The transducin γ-subunit from $Rce1^{-/-}$ retinal homogenates exhibited a reduced electrophoretic mobility (Fig. 3*A*), a characteristic of unprocessed forms of RCE1 substrates (7, 25). Although the steady-state levels of rhodopsin were reduced by 30% in *Rce1*-deficient retinas, the levels of the outer segment (OS) phototransduction proteins transducin, guanylate cyclase (GC-E), and arrestin, the OS structural protein peripherin, the inner segment (IS) protein AIPL1, and the bipolar cell proteins GOα and PKCα were unaffected by *Rce1* deficiency (Fig. 3*B*). Thus, the lack of light response in *Rce1*-deficient photoreceptor cells does not appear to be caused by changes in steady-state levels of prenylated RCE1 substrates.

***Rce1* Is Required for Intracellular Transport of PDE6.** We next tested if the absence of *Rce1* affected the transport of phototransduction proteins from the IS to the OS. We compared the localization of PDE6, Tγ, and GRK1 in $Rce1^{+/-}$ and $Rce1^{-/-}$ retinas by immunofluorescence. Cyclic nucleotide-gated channel α 1 (CNGA1) was used as a marker for the OS (31). In $Rce1^{+/-}$ retinas, the PDE6 β-subunit colocalized with CNGA1 in the OS (Fig. 4*A*). In contrast, the PDE6 β-subunit in $Rce1^{-/-}$ retinas did not colocalize with CNGA1 and could only be detected in the IS and ONL

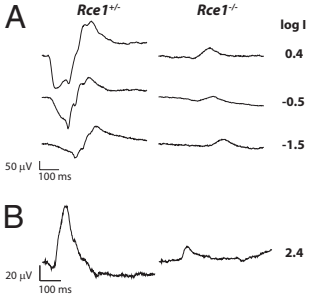

Fig. 2. Functional vision loss in mice lacking *Rce1* in the retina. (*A*) Scotopic ERG responses to increasing light intensities were recorded from P14 $Rce1^{+/-}$ and $Rce1^{-/-}$ littermates. Representative responses to log intensity (cd s^{-1}/m^2) flashes are shown. (*B*) Photopic ERG responses from $Rce1^{+/-}$ and $Rce1^{-/-}$ pups at log intensity 2.4 cd s^{-1}/m^2.

NEUROSCIENCE

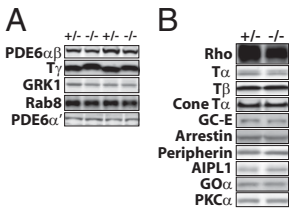

Fig. 3. Stability of prenylated proteins is maintained in the absence of RCE1-mediated endoproteolysis. Immunoblots of P8 *Rce1*$^{+/-}$ and *Rce1*$^{-/-}$ retinal lysates from littermates. Equal amounts of protein (150 μg) were loaded for each sample. (*A*) Western blots were probed with the indicated antibodies against prenylated proteins. Tγ displays a reduced electrophoretic mobility in *Rce1*$^{-/-}$ retinal lysates. (*B*) Levels of nonprenylated proteins of the retina were assessed in littermate pairs of P8 retinal lysates. PDE6αβ, cGMP phosphodiesterase 6; Tγ, transducin γ-subunit; GRK1, rhodopsin kinase; PDE6α′, cone cGMP phosphodiesterase; Rho, rhodopsin; Tα, transducin α-subunit; Tβ, transducin β-subunit; Cone Tα, cone transducin α-subunit; AIPL1, aryl hydrocarbon receptor interacting protein-like 1; GOα, guanine nucleotide-binding protein α-activating activity polypeptide O.

(Fig. 4*B*). No significant accumulation of PDE6 was observed in synaptic layer of photoreceptor cells (Fig. S6). The α- and γ-subunits of PDE6 were also confined to the IS and ONL in *Rce1*$^{-/-}$ retinas (Fig. S6). Our attempts to localize cone PDE6α′ was inconclusive as a result of rapid degeneration of photoreceptor cells (data not shown). The localizations of GRK1 and Tγ were unaffected by *Rce1* deficiency (Fig. 4 *C*–*F*). Moreover, GC-E, an OS integral membrane protein thought to be transported in association with PDE6, colocalized with CNGA1 in *Rce1*$^{-/-}$ retinas (32) (Fig. 4 *G* and *H*). These results suggest that unprocessed rod PDE6 subunits accumulate in the IS in *Rce1*$^{-/-}$ retinas and that their transport to the OS is blocked (Fig. 4*A*).

Normal Assembly and Activity of PDE6 in *Rce1*-Deficient Retina. Posttranslational modifications play a role in the assembly of multimeric proteins (33, 34). To determine if the absence of *Rce1* affected PDE6 assembly, we immunoprecipitated PDE6 heterotetramers with ROS1, a monoclonal antibody that only recognizes assembled PDE6. Immunoprecipitated proteins were separated on a SDS/PAGE gel followed by Western blotting using a polyclonal antibody that recognizes all three PDE6 subunits (35, 36). We found that *Rce1*$^{+/-}$ and *Rce1*$^{-/-}$ immunoprecipitation samples had similar levels of PDE6, indicating that the assembly of PDE6 multimers does not require *Rce1* (Fig. 5*A*).

To assess the ability of the assembled PDE6 enzyme to hydrolyze cGMP, we measured the enzymatic activity of PDE6 and the concentration of cGMP in the retina. These highly sensitive assays demonstrated that there were no significant differences in the ability of PDE6 in *Rce1*$^{+/-}$ and *Rce1*$^{-/-}$ retinas to hydrolyze cGMP. Consistent with our enzymatic assays, the level of cGMP was not significantly different in the presence or absence of RCE1 (Fig. 5 *B* and *C*).

Discussion

In this study, we show that the retina displays a unique requirement for RCE1-mediated endoproteolysis. *Rce1* is not needed for the development of retinal neurons but is specifically required for the maintenance of photoreceptor cells. *Rce1*$^{-/-}$ retinas exhibited minimal light responses, as measured by ERG, demonstrating the importance of postprenylation processing in phototransduction. The lack of light responses is likely a result of the mislocalization of PDE6, a prenylated protein complex critical to phototransduction. The data suggest that although the PDE6 heterotetramer is assembled and activated in the IS of *Rce1*$^{-/-}$ retinas, the complex fails to be transported to the photoreceptor cell OS.

Interestingly, despite the absence of *Rce1* from early stages of retinal development, we observed no deficits in the formation of

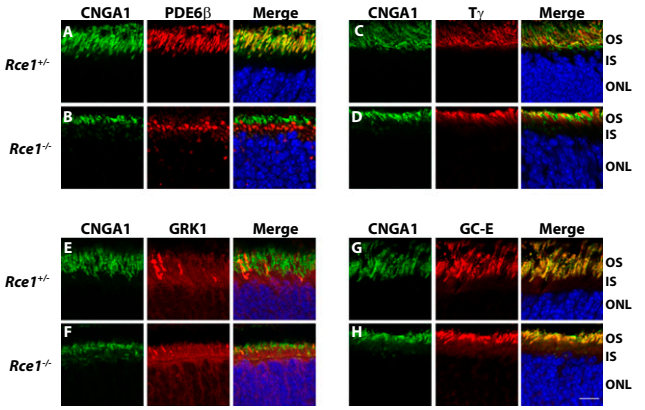

Fig. 4. Intracellular transport of PDE6 requires proteolysis by RCE1 for proper localization. Immunohistochemistry using indicated antibodies on cryosections from P12 retina. Nuclei are labeled by TO-PRO-3 and appear in blue. OSs are labeled with CNGA1 and appear in green. (*A*) Colocalization of PDE6 β-subunit and CNGA1 in the OS of photoreceptor cells from *Rce1*$^{+/-}$ retinal sections (red). (*B*) Mis-localization of PDE6 β-subunit in the IS of rod photoreceptor cells of *Rce1*$^{-/-}$ retinal sections (red). (*C* and *D*) Colocalization of Tγ and CNGA1 in the OS of photoreceptor cells in both *Rce1*$^{+/-}$ and *Rce1*$^{-/-}$ retinal sections (yellow). (*E* and *F*) Rhodopsin kinase (GRK1) is localized in the OS and IS equally between *Rce1*$^{+/-}$ and *Rce1*$^{-/-}$ retinas. (*G* and *H*) GC-E colocalizes with CNGA in the photoreceptor cell OS in both *Rce1*$^{+/-}$ and *Rce1*$^{-/-}$ retinas. (Scale bar: 10 μm.)

retinal cell layers at P8. At all tested ages, survival of the neurons in the inner retina was unaffected by the lack of *Rce1*. However, the photoreceptor cells in *Rce1*$^{-/-}$ retina do not survive beyond P30.

The rapid photoreceptor cell degeneration observed in *Rce1*$^{-/-}$ retinas is reminiscent of the photoreceptor cell loss seen in mice with mutations in PDE6 subunits, such as *rd*/*rd* mice, or in mice lacking *Aipl1* (30, 37). However, in these mice, photoreceptor cell degeneration was linked to the destabilization of PDE6 and subsequent accumulation of cGMP (37). In *Rce1*$^{-/-}$ retinas, by contrast, the stability of PDE6 was unaffected and cGMP levels were unchanged (Figs. 3*A* and 5*C*). In addition, loss of photoreceptor

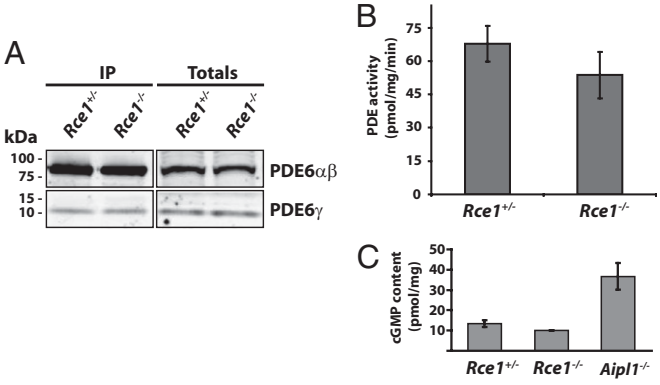

Fig. 5. PDE6 is assembled and functional in retina lacking *Rce1*. (*A*) Immunoprecipitation (IP) from P8 retinal extracts with ROS-1 monoclonal antibody. ROS-1 precipitates assembled PDE6 heteromer. Western blots of eluted IP extracts probed with MOE antibody that recognizes individual PDE6 subunits (α, β, γ). Total samples represent the input to each IP reaction. (*B*) Trypsin-activated PDE activity from P09 *Rce1*$^{+/-}$ and *Rce1*$^{-/-}$ retinal homogenates measured in triplicate. The difference in enzymatic activity between *Rce1*$^{+/-}$ and *Rce1*$^{-/-}$ retinas was not statistically significant ($P = 0.35$). (*C*) Competitive immunoassay for cGMP content (assay design) in P10 retinal extracts from *Rce1*$^{+/-}$, *Rce1*$^{-/-}$ and *Aipl1*$^{-/-}$ mice. No significant change in cGMP level was found between *Rce1*$^{+/-}$ and *Rce1*$^{-/-}$ retinal extracts ($P = 0.18$). However, cGMP level in *Aipl1*$^{-/-}$ retina was significantly higher ($P = 0.03$).

cells was not accompanied by reduced stability of any of the major phototransduction proteins except rhodopsin, which was reduced by 30%. It is unlikely that reduced rhodopsin levels in *Rce1*$^{-/-}$ retinas was the cause of the rapid photoreceptor cell degeneration, as a 50% reduction in rhodopsin levels leads to only a slow degeneration (38).

PDE6 does not seem to require RCE1 processing for catalytic activity as we observed only minor reductions in trypsin-activated cGMP hydrolytic activity in *Rce1*$^{-/-}$ retinas. Furthermore, cGMP level was not altered, consistent with the presence of functional PDE6 (Fig. 5*C*). At this point, the likeliest explanation for the photoreceptor cell dysfunction is that PDE6 accumulates in the IS and fails to reach its site of action in the OS. However, we cannot rule out the possibility that dysfunction of other prenylated photoreceptor cell signaling proteins are at the root of the phenotypes of *Rce1*-deficient retinas. This possibility seems unlikely, however, because the localization and stability of other prenylated substrates, including Tγ and GRK1, were unaffected by the absence of *Rce1*.

The OS is the default location for lipid-modified proteins, and the highly selective loss of PDE6 transport in *Rce1*-deficient retinas is intriguing (39). One potential explanation is that there is an active mechanism preventing the transport of unprocessed PDE6. Another is that RCE1-mediated endoproteolysis of a yet-unidentified CAAX protein is required for the transport of PDE6 following assembly in the IS. A third potential explanation is that the PDE6 transport mechanism requires that the carboxyl terminus of PDE6 is cleaved by RCE1 and methylated by ICMT. For example, the lack of RCE1-mediated proteolysis of PDE6 might disrupt its interaction with a protein binding partner or membrane domain in the IS that normally promotes the transport of PDE6 to the OS. PrBP/δ and AIPL1 are well known binding partners of PDE6 (40, 41). Previous studies have shown that the prenylcysteine methyl group of PDE6 peptides is important for the interaction with PrBP/δ (42). However, PrBP/δ-KO mice exhibit only a minor defect in rod PDE6 transport (32). AIPL1, on the contrary, is critical in early folding and assembly of PDE6 subunits (36, 37). PDE6 in *Rce1*$^{-/-}$ retinal homogenates could assemble into functional heterotetramers in the IS (Fig. 5*A*), suggesting that the interaction with AIPL1 is not affected. Thus, the mechanisms behind the selective loss of PDE6 transport remains to be determined.

The sequence of events from PDE6 synthesis to its insertion into the OS membrane is beginning to emerge. Our previous studies show that AIPL1 is involved in initial folding and/or assembly of PDE6 subunits (36). The present study clearly demonstrates that RCE1 is required for the transport of the fully assembled enzyme from the IS to the OS. Our model suggests that PDE6 subunits are assembled into a functional heterotetramer in the IS of the photoreceptor cell before being exported to the OS.

Materials and Methods

Animal Models. *Rce1*$^{fl/fl}$ mice were described previously (9, 25). To enhance the efficiency of recombination by Six3-*Cre*, we generated heterozygous *Rce1*$^{wt/null}$ mice by crossing *Rce1*$^{fl/fl}$ mice with transgenic mice expressing Cre under a ubiquitous *β-actin* promoter (43). *Rce1*$^{wt/null}$ mice developed normally and did not exhibit any visual deficits. The *Rce1*$^{wt/null}$ mice were crossed with *Six3-Cre* mice to obtain *Rce1*$^{wt/null}$Six3-*Cre* mice. These mice were then crossed with *Rce1*$^{fl/fl}$ mice for experimental and control samples. *Aipl1*$^{null/null}$ mice were previously described (37).

Message Analysis. Retinas, dissected from freshly enucleated eyes, were flash-frozen in dry ice in the presence of TRIzol (Invitrogen). RNA was extracted from frozen retinas and used to generate cDNA using SuperScript III (Invitrogen). Three hundred micrograms of cDNA from heterozygous and KO littermates in triplicate was used as a template for quantitative PCR using MyiQ PCR cycler (Bio-Rad) and MyiQ SYBR Green Supermix (Bio-Rad). *Rce1* was amplified using primers 5′-AGTGTGGGAAGTATCTTCGTGTCT-3′ and 5′-CTGTTCTTTCCAAAAGCATACAAA-3′ to generate a 289-bp product. Zinc metalloproteinase sterile 24 (*Zmpste24*), the homologue of *Rce1*, was amplified using primers 5′-TGCCTGGCTGTTCACATTAG-3′ and 5′-TCACTGTCCCCTTCACCTTC-3′ to generate a 336-bp product. Threshold values were normalized to hypoxanthine phosphoribosyltransferase (*Hprt*) gene expression levels with the primers 5′-CAAACTTTGCTTTCCCTGGT-3′ and 5′-CAAGGGCATATCCAACAACA-3′ (250-bp product).

Histology. Mice were euthanized by CO_2 inhalation, and eyes were enucleated. A 2-mm hole was made at the corneal limbus and eyes were fixed (1.6% paraformaldehyde, 2.5% glutaraldehyde, 0.05% $MgCl_2$, 0.04 M sucrose in 0.08 M Pipes buffer, pH 7.0) for 5 min before dissecting the anterior chamber and removing the lens. Eyecups for semithin plastic sections were prepared according to JB-4 (Electron Microscopy Sciences) embedding protocol. In brief, eyecups were fixed for 12 h at 4 °C. Following a 30-min wash in PBS solution, eyecups were dehydrated in a graded alcohol series. Two changes of infiltration solution were performed before an overnight incubation in fresh infiltration solution. Eyecups were embedded in JB-4 in a BEEM capsule (Electron Microscopy Sciences) on ice. Sections (3 μm) were cut on a Leica ultramicrotome and mounted on Superfrost plus slides (Fisher Scientific). H&E staining was carried out by the West Virginia University pathology department, and images were captured on an Olympus AX70 transmitted light microscope.

Immunohistochemistry. Eyecups for cryosections were dissected as previously stated, then fixed for 2 h in 4% paraformaldehyde in PBS solution before cryoprotection in 30% sucrose overnight at 4 °C. Eyecups were embedded in Tissue-Tek optimal cutting temperature compound (Sakura) and fast-frozen in dry ice ethanol bath. Blocks were sectioned with a Leica CM1850 Cryostat and 15- to 20-μm sections were mounted on Superfrost plus slides. Cryosections were washed in PBS solution, and then incubated in blocking buffer [2% goat serum (Invitrogen), 0.1% Triton X-100, and 0.05% sodium azide in PBS solution] for 1 h. Primary antibodies were incubated for 2 h at room temperature or overnight at 4 °C. Excess antibody was removed by three 10-min washes in PBS solution with 0.1% Triton X-100 before incubation with secondary antibody for 1 h at room temperature. Slides were washed twice for 10 min with PBS solution with 0.1% Triton X-100 and for 10 min in PBS solution. ProLong Gold antifade reagent (Invitrogen) was applied to each section, and then coverslips were mounted. Images were collected on a Zeiss LSM 510 Meta confocal microscope using 488-, 543-, and 633-nm laser lines. The following antibodies were used: anti-CNGA1/3 (University of California, Davis/National Institutes of Health NeuroMab Facility), anti-PDE β (Affinity Bioreagents), anti-Tγ (Santa Cruz), anti-GRK1 (Ching-Kang Chen, Virginia Commonwealth University, Richmond, VA), and anti-GC-E (David Garbers, deceased; University of Texas Southwestern Medical School, Dallas, TX). TO-PRO-3 nuclear stain (Invitrogen) was added to dilutions of Alexa Fluor secondary antibodies (Invitrogen) in antibody dilution buffer (0.05% goat serum, 0.1% Triton X-100, and 0.05% sodium azide in 1× PBS solution).

ERG. Littermates were dark-adapted overnight, then eyes were dilated (1:1 phenylephrine:tropicamide) for 10 min. Isoflurane anesthesia (1.5% in 2.5% oxygen) was administered via nose cone on a 37 °C platform. A reference electrode was placed s.c. in the scalp and silver wire electrodes were positioned above the cornea, with contact being made by methylcellulose solution. Light flashes were presented by placing the mouse in a Ganzfeld apparatus. Corneal evoked potentials were collected using UTAS-E4000 Visual Electrodiagnostic Test System and EMWIN 8.1.1 software (LKC Technologies). Background light (30 cd·m^{-2}) was presented for 10 min before recording flicker responses in the presence of the background light. Grabdata (Machelle Pardue, Emory University) was used to import raw data into Excel (Microsoft) for final analysis of response curves. Representative waveforms are shown.

Immunoblot. Flash-frozen retinal samples were solubilized in 6 M urea buffer (6 M urea, 4% SDS, 0.5 M Tris, pH 6.8, 10 mg/mL DTT, and 2% bromophenol blue) using sonication for six pulses of 20 ms at power setting 6 (XL-2000; Misonix). The protein concentration was estimated by using a NanoDrop (Thermo Scientific) spectrophotometer. Total protein samples (150 μg) were resolved on 4% to 20% Criterion (Bio-Rad) polyacrylamide gels. Proteins were then transferred to Immobilon-FL membrane (Millipore) and probed with primary antibodies against desired target proteins. The following antibodies were used: anti-PDE6αβγ (MOE; Cytosignal), anti-Tγ (Santa Cruz), anti-GRK1 (Thermo Fisher), anti-Rab8 (BD Bioscience), anti-PDE6α′ (44), anti-Rhodopsin (Robert Molday, University of British Columbia, Vancouver, BC, Canada), anti-Tα (Santa Cruz), anti-Tβ (Affinity Bioreagents), anti-Cone Tα (Santa Cruz), anti-GC-E (James Hurley, University of Washington, Seattle, WA), anti-arrestin (Affinity Bioreagents), anti-peripherin (Gabriel Travis, University of California, Los Angeles, CA), anti-AIPL1 (45), anti-GOα (Santa Cruz), and anti-PKCα (Affinity Bioreagents). Odyssey goat anti-rabbit Alexa 680 and Odyssey goat anti-mouse Alexa 680 secondary antibodies (LI-COR Biosciences) were used at 1:50,000 dilutions to label primary antibodies. Membranes were scanned

with an Odyssey Infrared Imaging System (LI-COR Biosciences). Images are representative of at least three independent experiments.

Immunoprecipitation. PDE6 assembly was assessed by immunoprecipitation with ROS-1 monoclonal antibody (Joseph Beavo, University of Washington, Seattle, WA) as previously described (36). Briefly, retinas were homogenized in PBS solution containing Complete Mini EDTA-Free protease inhibitor tablet (Roche) using a pellet pestle (VWR) in an Eppendorf tube on ice. To solubilize the proteins, 1% Triton X-100 was added and samples were nutated for 30 min at 4 °C. Samples were clarified by centrifugation for 5 min at 10,000 × *g*. Supernatants from the previous centrifugation step were incubated with ROS-1–coupled Protein A/G beads for 3 h. Unbound proteins were removed and beads were washed in Triton buffer (1% Triton X-100, 50 mM Tris, pH 7.5, 300 mM NaCl, 5 mM EDTA, 0.02% NaN_3). PDE6 subunits bound to ROS-1 were eluted from the beads by adding SDS/PAGE sample buffer (62.5 mM Tris, pH 6.8, 2% SDS, 10% glycerol, 0.005% bromophenol blue, 5% 2-mercaptoethanol) and boiling for 5 min. Eluates were resolved on polyacrylamide gels and immunblotted as described earlier with MOE antibody (1:4,000), which recognizes rod PDE6 α-, β-, and γ-subunits.

PDE Activity Assay. cGMP hydrolysis by trypsin-activated PDE6 was performed as previously described (37, 46, 47). Briefly, two retinas were homogenized with a pellet-pestle (VWR) in 100 μL ROS buffer (20 mM Hepes, pH 7.2, 2 mM $MgCl_2$, 60 mM KCl, 30 mM NaCl, 1 mM DTT, 0.1 mM ATP). Five micrograms of retinal homogenate was treated with trypsin (Sigma), final concentration 40 μg/mL, at room temperature for 2 min. Reactions were stopped by the addition of fivefold excess of soybean trypsin inhibitor (Sigma). Hydrogen 3-labeled cGMP (Perkin-Elmer) in Tris-buffered cGMP (100 mM Tris, pH 8.0, 4.8 mM $MgCl_2$, 60 mM cGMP) was added to each sample and incubated at 30 °C for 4 min before boiling for 3 min. Snake venom (Sigma) was then added to each reaction for 15 min at 30 °C to cleave the phosphate group from 5′ GMP. Samples were mixed with a Dowex (Sigma) ion exchange column and incubated for 30 min (47). After centrifugation, the supernatant was added to scintillation fluid and counted on a Wallac 1410 liquid scintillation counter.

cGMP Assay. Two retinas per sample were homogenized in 0.1 N HCl, and protein concentration was estimated by using a NanoDrop spectrophotometer. Retinal homogenates were boiled for 5 min and clarified by centrifugation at 6,000 × *g* for 5 min at 4 °C. Supernatant was neutralized in 0.5 M Tris, pH 8.0. Equal amounts of samples (1 mg of total protein) were used to measure cGMP levels using the Direct cGMP enzyme immunoassay kit (Assay Designs) as described by the manufacturer.

ACKNOWLEDGMENTS. We thank Dr. Peter Mathers for the experimental advice and generous sharing of mice and Dr. Karen Martin for advice and the use of the West Virginia University Microscopic Imaging Facility. For critical reading of the manuscript, we thank Drs. Lori Kang and James Hurley. We would also like to thank the members of the Ramamurthy laboratory. We thank Drs. Ariel Agmon, Joseph Beavo, David Garbers, James Hurley, Robert Molday, Gabriel Travis, and Theodore Wensel for their generous donation of reagents. This work was supported by National Institutes of Health Grants R01EY017035 (to V.R.) and P30RR031155 (to George Spirou), West Virginia Lions, and an Unrestricted Research to Prevent Blindness challenge grant (West Virginia University).

1. Glomset JA, Gelb MH, Farnsworth CC (1990) Prenyl proteins in eukaryotic cells: A new type of membrane anchor. *Trends Biochem Sci* 15:139–142.
2. Zhang FL, Casey PJ (1996) Protein prenylation: Molecular mechanisms and functional consequences. *Annu Rev Biochem* 65:241–269.
3. Lane KT, Beese LS (2006) Thematic review series: Lipid posttranslational modifications. Structural biology of protein farnesyltransferase and geranylgeranyltransferase type I. *J Lipid Res* 47:681–699.
4. Wright LP, Philips MR (2006) Thematic review series: Lipid posttranslational modifications. CAAX modification and membrane targeting of Ras. *J Lipid Res* 47:883–891.
5. Barrowman J, Michaelis S (2009) ZMPSTE24, an integral membrane zinc metalloprotease with a connection to progeroid disorders. *Biol Chem* 390:761–773.
6. Michaelson D, et al. (2005) Postprenylation CAAX processing is required for proper localization of Ras but not Rho GTPases. *Mol Biol Cell* 16:1606–1616.
7. Kim E, et al. (1999) Disruption of the mouse Rce1 gene results in defective Ras processing and mislocalization of Ras within cells. *J Biol Chem* 274:8383–8390.
8. Bergo MO, et al. (2001) Isoprenylcysteine carboxyl methyltransferase deficiency in mice. *J Biol Chem* 276:5841–5845.
9. Bergo MO, et al. (2004) On the physiological importance of endoproteolysis of CAAX proteins: Heart-specific RCE1 knockout mice develop a lethal cardiomyopathy. *J Biol Chem* 279:4729–4736.
10. Wahlstrom AM, et al. (2007) Rce1 deficiency accelerates the development of K-RAS-induced myeloproliferative disease. *Blood* 109:763–768.
11. Swanson RJ, Applebury ML (1983) Methylation of proteins in photoreceptor rod outer segments. *J Biol Chem* 258:10599–10605.
12. Qin N, Baehr W (1994) Expression and mutagenesis of mouse rod photoreceptor cGMP phosphodiesterase. *J Biol Chem* 269:3265–3271.
13. Ong OC, Ota IM, Clarke S, Fung BK (1989) The membrane binding domain of rod cGMP phosphodiesterase is posttranslationally modified by methyl esterification at a C-terminal cysteine. *Proc Natl Acad Sci USA* 86:9238–9242.
14. Fukada Y, et al. (1990) Farnesylated gamma-subunit of photoreceptor G protein indispensable for GTP-binding. *Nature* 346:658–660.
15. Anant JS, et al. (1992) In vivo differential prenylation of retinal cyclic GMP phosphodiesterase catalytic subunits. *J Biol Chem* 267:687–690.
16. Inglese J, Koch WJ, Caron MG, Lefkowitz RJ (1992) Isoprenylation in regulation of signal transduction by G-protein-coupled receptor kinases. *Nature* 359:147–150.
17. Burns ME, Arshavsky VY (2005) Beyond counting photons: Trials and trends in vertebrate visual transduction. *Neuron* 48:387–401.
18. Michaelson D, Ahearn I, Bergo M, Young S, Philips M (2002) Membrane trafficking of heterotrimeric G proteins via the endoplasmic reticulum and Golgi. *Mol Biol Cell* 13:3294–3302.
19. Fukada Y, et al. (1994) Effects of carboxyl methylation of photoreceptor G protein gamma-subunit in visual transduction. *J Biol Chem* 269:5163–5170.
20. Wensel TG (2008) Signal transducing membrane complexes of photoreceptor outer segments. *Vision Res* 48:2052–2061.
21. Suber ML, et al. (1993) Irish setter dogs affected with rod/cone dysplasia contain a nonsense mutation in the rod cGMP phosphodiesterase beta-subunit gene. *Proc Natl Acad Sci USA* 90:3968–3972.
22. Muradov H, Boyd KK, Artemyev NO (2010) Rod phosphodiesterase-6 PDE6A and PDE6B subunits are enzymatically equivalent. *J Biol Chem* 285:39828–39834.
23. Pittler SJ, Fliesler SJ, Fisher PL, Keller PK, Rapp LM (1995) In vivo requirement of protein prenylation for maintenance of retinal cytoarchitecture and photoreceptor structure. *J Cell Biol* 130:431–439.
24. Kramer K, et al. (2003) Isoprenylcysteine carboxyl methyltransferase activity modulates endothelial cell apoptosis. *Mol Biol Cell* 14:848–857.
25. Bergo MO, et al. (2002) Absence of the CAAX endoprotease Rce1: Effects on cell growth and transformation. *Mol Cell Biol* 22:171–181.
26. Furuta Y, Lagutin O, Hogan BL, Oliver GC (2000) Retina- and ventral forebrain-specific Cre recombinase activity in transgenic mice. *Genesis* 26:130–132.
27. Madisen L, et al. (2010) A robust and high-throughput Cre reporting and characterization system for the whole mouse brain. *Nat Neurosci* 13:133–140.
28. Nusinowitz S, Ridder WH, Heckenlively JR (2002) Electrophysiological testing of the mouse visual system. *Systematic Evaluation of the Mouse Eye*, ed Smith RS (CRC Press, Boca Raton, FL), pp 320–344.
29. Lobanova ES, et al. (2008) Transducin gamma-subunit sets expression levels of alpha- and beta-subunits and is crucial for rod viability. *J Neurosci* 28:3510–3520.
30. Farber DB (1995) From mice to men: The cyclic GMP phosphodiesterase gene in vision and disease. The Proctor Lecture. *Invest Ophthalmol Vis Sci* 36:263–275.
31. Molday RS, et al. (1991) The cGMP-gated channel of the rod photoreceptor cell characterization and orientation of the amino terminus. *J Biol Chem* 266:21917–21922.
32. Zhang H, et al. (2007) Deletion of PrBP/delta impedes transport of GRK1 and PDE6 catalytic subunits to photoreceptor outer segments. *Proc Natl Acad Sci USA* 104:8857–8862.
33. Winter-Vann AM, Casey PJ (2005) Post-prenylation-processing enzymes as new targets in oncogenesis. *Nat Rev Cancer* 5:405–412.
34. Marrari Y, Crouthamel M, Irannejad R, Wedegaertner PB (2007) Assembly and trafficking of heterotrimeric G proteins. *Biochemistry* 46:7665–7677.
35. Hurwitz RL, Bunt-Milam AH, Beavo JA (1984) Immunologic characterization of the photoreceptor outer segment cyclic GMP phosphodiesterase. *J Biol Chem* 259:8612–8618.
36. Kolandaivelu S, Huang J, Hurley JB, Ramamurthy V (2009) AIPL1, a protein associated with childhood blindness, interacts with {alpha}-subunit of rod phosphodiesterase (PDE6) and is essential for its proper assembly. *J Biol Chem* 284:30853–30861.
37. Ramamurthy V, Niemi GA, Reh TA, Hurley JB (2004) Leber congenital amaurosis linked to AIPL1: A mouse model reveals destabilization of cGMP phosphodiesterase. *Proc Natl Acad Sci USA* 101:13897–13902.
38. Lem J, et al. (1999) Morphological, physiological, and biochemical changes in rhodopsin knockout mice. *Proc Natl Acad Sci USA* 96:736–741.
39. Baker SA, et al. (2008) The outer segment serves as a default destination for the trafficking of membrane proteins in photoreceptors. *J Cell Biol* 183:485–498.
40. Gillespie PG, Prusti RK, Apel ED, Beavo JA (1989) A soluble form of bovine rod photoreceptor phosphodiesterase has a novel 15-kDa subunit. *J Biol Chem* 264:12187–12193.
41. Kolandaivelu S, Huang J, Hurley JB, Ramamurthy V (2009) AIPL1, a protein associated with childhood blindness, interacts with alpha-subunit of rod phosphodiesterase (PDE6) and is essential for its proper assembly. *J Biol Chem* 284:30853–30861.
42. Cook TA, Ghomashchi F, Gelb MH, Florio SK, Beavo JA (2000) Binding of the delta subunit to rod phosphodiesterase catalytic subunits requires methylated, prenylated C-termini of the catalytic subunits. *Biochemistry* 39:13516–13523.
43. Meyers EN, Lewandoski M, Martin GR (1998) An Fgf8 mutant allelic series generated by Cre- and Flp-mediated recombination. *Nat Genet* 18:136–141.
44. Kirschman LT, et al. (2010) The Leber congenital amaurosis protein, AIPL1, is needed for the viability and functioning of cone photoreceptor cells. *Hum Mol Genet* 19:1076–1087.
45. Ramamurthy V, et al. (2003) AIPL1, a protein implicated in Leber's congenital amaurosis, interacts with and aids in processing of farnesylated proteins. *Proc Natl Acad Sci USA* 100:12630–12635.
46. Hurley JB, Stryer L (1982) Purification and characterization of the gamma regulatory subunit of the cyclic GMP phosphodiesterase from retinal rod outer segments. *J Biol Chem* 257:11094–11099.
47. MacKenzie SJ, Hastings SF, Wells C (2010) Cyclic nucleotide phosphodiesterase assay technology. *Current Protocols in Pharmacology* (Wiley, New York), pp 3.12.11–13.12.26.